Electronic Materials Letters, Vol. 4, No. 2 (2008), pp. 75-77

Formation of Nanoporous Pt Thin Films by Electrochemical Dissolution

Chunjoong Kim, Yejun Park, Changwoo Nahm, and Byungwoo Park*

Department of Materials Science and Engineering, and Research Center for Energy Conversion and Storage, Seoul National University, Seoul 151-744, Korea

To study nanoporous formation by electrochemical dissolution, $Pt_{0.52}Al_{0.48}$ thin films were examined during 500 repeated cycles. Although the $Pt_{0.52}Al_{0.48}$ thin films exhibited similar electrocatalytic properties to Pt thin films at the initial stages, the $Pt_{0.52}Al_{0.48}$ thin films showed gradually increasing electrocatalytic properties as cycles proceeded. These enhancements are attributed to the nanoporosities in the $Pt_{0.52}Al_{0.48}$ thin films. The nanoporous Pt thin films, after the complete dissolution of Al, exhibited approximately one order of magnitude larger electrochemical surface area than Pt thin films. Superior methanol-oxidation activities were also observed in the nanoporous Pt thin films.

Keywords: nanostructures, nanoporosity, dissolution, platinum

1. INTRODUCTION

Among the various energy conversion and storage devices, proton-exchange-membrane fuel cells (PEMFCs) are promising alternatives for the next-generation power sources due to advantages that include high-energy efficiency, zero emission, and low-temperature operation (<100°C).[1-3] Despite significant progress in PEMFC development, barriers remain to the wide use of PEMFCs, such as inefficient utilization of catalysts, low oxygen-reduction reaction (ORR), loss of Pt activity over long-term operation, and easy poisoning by CO, in addition to the economic barrier.[4,5] To resolve these issues, various nanostructured electrocatalysts have been intensively investigated.[6-10] Especially, porous electrocatalysts have shown enhanced catalytic activities compared with bulk Pt,[11,12] because the porous materials are greatly advantageous as catalysts or electrodes, due to the large reaction sites and short diffusion paths for reactants.[13-15]

Al is unsuitable for electrocatalysts in PEMFCs due to its instability in an acidic condition and much lower redox potential ($Al \leftrightarrow Al^{3+} + 3e^-$, E^o = -1.61 V vs. NHE at pH 1) than the potential window of PEMFCs (0 – 1.23 V). However, the instability of Al can be effectively utilized to synthesize the nanoporous structure of Pt. By repeated voltage sweeps with proper scan rates, nanoporous Pt thin films could be easily synthesized by the selective dissolution of Al from the $Pt_{0.52}Al_{0.48}$ thin films. Nanoporous Pt thin films show enhanced methanol-oxidation activities.

In this letter, Pt nanoporous thin films were synthesized through the selective dissolution of Al in the $Pt_{0.52}Al_{0.48}$ thin films, and their electrocatalytic activities were examined. After the dissolution of Al, nanoporous Pt thin films showed one order of magnitude higher catalytic activities compared with the untreated Pt thin films.

*Corresponding author: byungwoo@snu.ac.kr

2. EXPERIMENTAL PROCEDURE

The $Pt_{0.52}Al_{0.48}$ thin films were deposited on Si(100) substrates by rf magnetron sputtering using Pt and Al targets. Sputtering was performed under an Ar atmosphere with a flow rate of 30 sccm with an operating pressure of 10 mTorr at 400°C. The sputtering powers of the Al and Pt were fixed at 50 W.

Electrochemical measurements were made using a conventional three-electrode electrochemical system at room temperature (RT). The $Pt_{0.52}Al_{0.48}$ thin-film electrodes, Pt wire, and saturated calomel electrode were used as the working electrode, counter electrode, and reference electrode, respectively. The electrochemical properties of the $Pt_{0.52}Al_{0.48}$, Pt, and Al thin-film electrodes were determined by cyclic voltammograms (*CV*s) at potentials ranging from 0.03 to 1.03 V at a scan rate of 100 mV/s in aqueous sulfuric acid (0.5 M H_2SO_4). The methanol-oxidation activities on these electrodes were investigated in a solution of 0.5 M H_2SO_4 and 2 M CH_3OH. All the solutions were purged with N_2 gas for 30 min before each electrochemical measurement. The changes of electrochemical surface area (*ESA*) of the $Pt_{0.52}Al_{0.48}$ and Pt thin films were determined using a hydrogen-desorption method Pt-H.[16]

The nanostructures of the $Pt_{0.52}Al_{0.48}$ thin films were analyzed by x-ray diffraction (XRD). The atomic ratio of Pt and

Al was measured by inductively coupled plasma-atomic emission spectroscopy (ICP-AES). The chemical-bond states of the Pt and Al were analyzed by x-ray photoelectron spectroscopy (XPS).

3. RESULTS AND DISCUSSION

Figure 1 shows the cyclic voltammograms of the $Pt_{0.52}Al_{0.48}$, Pt, and Al thin films during 500 cycles. At the initial stage, $Pt_{0.52}Al_{0.48}$ thin films exhibited similar catalytic activities to the bare Pt thin films. However, as cycles proceeded, the $Pt_{0.52}Al_{0.48}$ thin films showed gradually enhanced catalytic activities. While the initial *ESA* of $Pt_{0.52}Al_{0.48}$ was 1.78 cm^2 (per 1 cm^2 sample), the *ESA* at the 500 cycles was 16.42 cm^2 (per 1 cm^2 sample). The increased *ESA* is attributed to nanoporosities, which are formed by the gradual dissolution of Al. Although the redox potential of Al at pH 1 is -1.61 V ($Al \leftrightarrow Al^{3+} + 3e^-$), the dissolution of Al initiates at ~0.68 V due to the low kinetics of Al dissolution, as shown in Fig. 1.[17] Furthermore, Al thin films show much faster dissolution compared with the $Pt_{0.52}Al_{0.48}$ thin films, because Pt atoms act as diffusion barriers for Al dissolution into the electrolytes.[18,19]

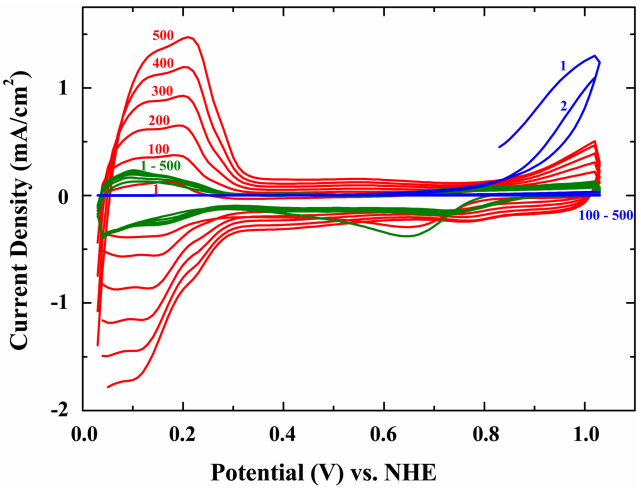

Fig. 1. (Color) Cyclic voltammograms of the $Pt_{0.52}Al_{0.48}$ (red), Pt (green), and Al (blue) thin films during 500 cycles. *CV*s were carried out in a 0.5 M H_2SO_4 solution at a scan rate of 100 mV/s.

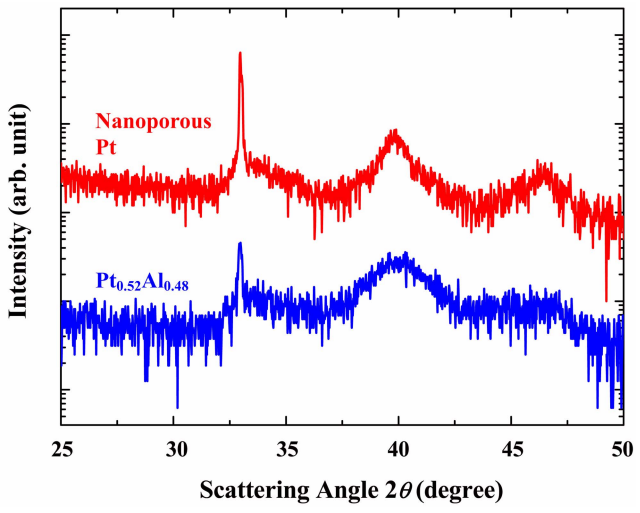

Fig. 2. (Color) XRD patterns of as-deposited $Pt_{0.52}Al_{0.48}$ and nanoporous Pt thin films (after 500 cycles).

X-ray diffraction (XRD) patterns for as-deposited $Pt_{0.52}Al_{0.48}$ (before 500 cycles) and nanoporous Pt thin films (after 500 cycles) are shown in Fig. 2. As seen in Fig. 2, $Pt_{0.52}Al_{0.48}$ thin films show mixed phases of intermetallic compounds. However, only crystalline Pt, with the size of ~4 nm, is observed in the nanoporous Pt thin films (after 500 cycles). ICP-AES analysis also showed that no Al remained in the $Pt_{0.52}Al_{0.48}$ thin films after 500 cycles.

Figure 3 shows the total reflection spectra of the $Pt_{0.52}Al_{0.48}$ and nanoporous Pt thin films. The thicknesses and densities of the thin films are simulated from the reflection spectra. The nanoporous Pt thin films exhibited decreased density (~50% of Pt) by dissolution of Al from the $Pt_{0.52}Al_{0.48}$ thin films, as confirmed by XRD and ICP-AES.

XPS spectra for the Al 2*s* and Pt 4*f* core levels of the $Pt_{0.52}Al_{0.48}$ thin films and nanoporous Pt thin films confirmed

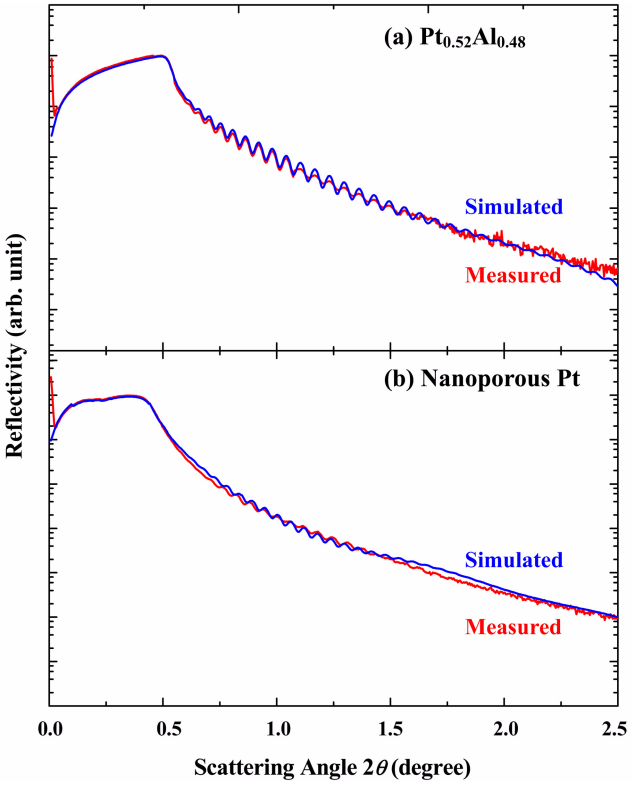

Fig. 3. (Color) The total reflection spectra in XRD of the (a) $Pt_{0.52}Al_{0.48}$ and (b) nanoporous Pt thin films. Simulated spectra (blue) are also shown with the measured spectra (red).

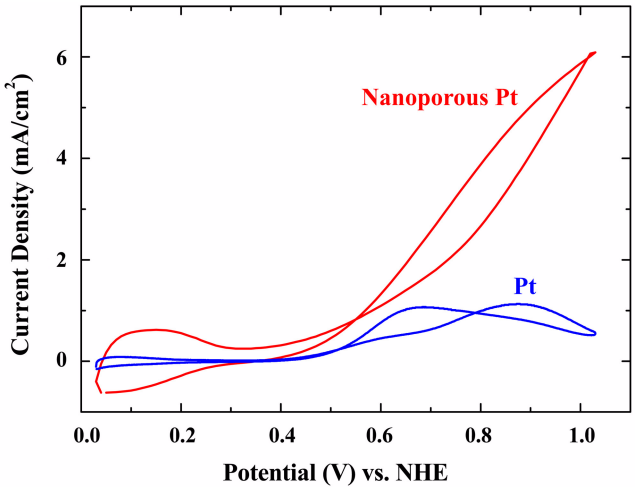

Fig. 4. (Color) Methanol-oxidation activities of nanoporous Pt (red) and Pt (blue) thin films. *CV*s were carried out in a 0.5 M H_2SO_4 and 2 M CH_3OH solution at a scan rate of 100 mV/s.

that the Pt 4*f* peaks of $Pt_{0.52}Al_{0.48}$ and nanoporous Pt thin films were zero-valent metallic Pt phases.[20-22] The Al 2*s* peaks correlated with metallic, and oxidized Al were observed only in the thin films before *CV*s. These spectral changes indicated a complete dissolution of Al in the $Pt_{0.52}Al_{0.48}$ thin films after the 500 cycles, which is consistent with the change of XRD patterns, as shown in Figs. 2 and 3.

Nanoporous thin films have shorter effective diffusion lengths for ionic species, and larger surface areas compared with bulk materials. These benefits are greatly advantageous to the electrocatalysts for methanol oxidation. The methanol-oxidation activities of these nanoporous thin films were investigated with a scan rate of 100 mV/s in a solution of 0.5 M H_2SO_4 and 2 M CH_3OH, as shown in Fig. 4. The nanoporous Pt thin films show higher methanol-oxidation activities compared with the untreated Pt. These results showed the potential application of nanoporous Pt thin films as a high-efficient catalyst for direct methanol fuel cells.

4. CONCLUSIONS

$Pt_{0.52}Al_{0.48}$ thin films exhibited similar electrocatalytic properties to bare Pt, while demonstrating gradually increasing catalytic activities during electrochemical cycles. It is believed that the electrochemical dissolution of Al under suitable conditions plays an important role in forming nanoporous Pt thin films. Nanoporous Pt thin films showed one order of magnitude higher catalytic activities compared with the untreated Pt thin films. The simple process developed in this study, which electrochemically dissolves Al in the $Pt_{0.52}Al_{0.48}$ thin films through the proper potential sweeps, can be easily applied to synthesizing nanoporous Pt in the bulk geometry. The electrocatalytic activities can be increased further by optimizing the nanostructured $Pt_{0.52}Al_{0.48}$ thin films.

ACKNOWLEDGMENT

This work was supported by the ERC program of MOST/KOSEF (R11-2002-102-00000-0).

REFERENCES

1. B. C. H. Steele and A. Heinzel, *Nature* **414**, 345 (2001).
2. Y. Oh, J.-G. Lee, B. Kim, and B. Park, *Electron. Mater. Lett.* **4**, 9 (2008); J.-G. Lee, C. Kim, B. Kim, D. Son, and B. Park, *Electron. Mater. Lett.* **2**, 111 (2006).
3. J. Cho, Y.-W. Kim, B. Kim, J.-G. Lee, and B. Park, *Angew. Chem. Int. Ed.* **42**, 1618 (2003); J. Cho, H. Kim, and B. Park, *J. Electrochem. Soc.* **151**, A1707 (2004); J.-G. Lee, B. Kim, J. Cho, Y.-W. Kim, and B. Park, *J. Electrochem. Soc.* **151**, A801 (2004).
4. L. D. Burke and J. F. Rohan, *J. Electrochem. Soc.* **139**, 1600 (1992).
5. M. L. Sattler and P. N. Ross, *Ultramicroscopy* **20**, 21 (1986).
6. C. Kim, B. Lee, Y. Park, B. Park, J. Lee, and H. Kim, *Appl. Phys. Lett.* **91**, 113101 (2007).
7. S. H. Joo, S. J. Choi, I. Oh, J. Kwak, Z. Liu, O. Teraski, and R. Ryoo, *Nature* **412**, 169 (2001).
8. F. Maillard, G.-Q. Lu, A. Wieckowski, and U. Stimming, *J. Phys. Chem. B.* **109**, 16230 (2005).
9. B. Lee, C. Kim, Y. Park, T.-G. Kim, and B. Park, *Electrochem. Solid-State Lett.* **9**, E27 (2006).
10. C. Nahm, C. Kim, Y. Park, B. Lee, and B. Park, *Electron. Mater. Lett.* **4**, 5 (2008).
11. K.-S. Choi, E. W. McFarland, and G. D. Stucky, *Adv. Mater.* **15**, 2018 (2003).
12. H.-P. Liang, H.-M. Zhang, J.-S. Hu, Y.-G. Guo, L.-J. Wan, and C.-Li Bai, *Angew. Chem. Int. Ed.* **43**, 1540 (2004).
13. D. Son, E. Kim, T.-G. Kim, J. Cho, B. Park, K. S. Ryu, and S. H. Chang, *Angew. Chem. Int. Ed.* **43**, 5987 (2004).
14. J.-G. Lee, D. Son, C. Kim, and B. Park, *J. Power Sources* **172**, 908 (2007).
15. Y.-S. Hu, Y.-G. Guo, W. Sigle, S. Hore, P. Balaya, and J. Maier, *Nature Mater.* **5**, 713 (2006).
16. T. J. Schmidt, H. A. Gasteiger, G. D. Stäb, P. M. Uraban, D. M. Kolb, and R. J. Behm, *J. Electrochem. Soc.* **145**, 2354 (1998).
17. D. A. Jones, in *Principles and Prevention of Corrosion*, *2nd ed.*, p. 50, Prentice Hall, NJ (1996).
18. J. Erlebacher, *J. Electrochem. Soc.* **151**, C614 (2004).
19. A. Bonakdarpour, R. Löbel, R. T. Atanasoski, G. D. Vernstrom, A. K. Schmoeckel, M. K. Debe, and J. R. Dahn, *J. Electrochem. Soc.* **153**, A1835 (2006).
20. G. E. McGuire, G. K. Schweitzer, and T. A. Carlson, *Inorg. Chem.* **12**, 2450 (1973).
21. J. F. Moulder, W. F. Stickle, P. E. Sobol, and K. D. Bomben, *Handbook of X-Ray Photoelectron Spectroscopy*, p. 54, Perkin-Elmer Corporation (1992).
22. E. Choi, S.-J. Oh, and M. Choi, *Phys. Rev. B.* **43**, 6360 (1991).